TWO-TEMPERATURE CHEMICAL-NONEQUILIBRIUM MODELLING OF THE HYDROGEN PLASMA FLOW IN A LOW-POWER ARCJET THRUSTER

W. P. SUN AND H. X. WANG*

School of Astronautics, Beijing University of Aeronautics and Astronautics, 100191, Beijing, China
*whx@buaa.edu.cn

ABSTRACT

A numerical simulation has been performed of a high-velocity hydrogen plasma arc flow in a low power arcjet including a finite-rate chemical kinetic model. Modelling results are found to compare favourably with available experimental data for the arcjet thrusters. The distributions of temperature and mole fraction of each species along the axis under three different working conditions have been calculated to investigate the effects of the arc current and the mass flow rate on the thermal and chemical nonequilibrium. The results show that the smaller arc current and larger mass flow rate increase the differences between the temperatures of electron and heavy-species and the degree of ionization and dissociation usually lags behind the values that would correspond to the rising or decreasing electron temperature.

1. INTRODUCTION

Arcjet is a thruster that heats a propellant stream by passing an electrical arc through it, before the propellant is expanded through divergent section of the nozzle to generate thrust. It could provide a substantial cost reduction for orbital transfer and station keeping missions, if electrically powered arcjets could be designed to have high specific impulse and good thermal efficiency. Understanding the details of flowfield inside the arcjet thruster is necessary for fundamental research as well as for further optimization of these devices.

In order to predict the main plasma flow features and arcjet performance, the assumption of local thermodynamic equilibrium (LTE) in thermal plasmas has been successfully used both in simulations[1,2] and in the interpretation of experimental data. Within the arcjet, the propellant is heated rapidly in the constrictor and then expanded in the expansion portion of the thruster nozzle to a high velocity. These processes in such a small space cause large gradients of temperature and velocity, which may result in the departures from the LTE. This important phenomenon in thermal plasma processing has attracted more and more researchers to study deeply, since they have strong effects on both the plasma flow and the heating of entrained particles. In this paper, numerical simulation based on the two temperatures and finite chemical reaction rate assumption is conducted.

2. MODELLING APPROACH

The main assumptions employed in the modelling study are as follows, (i) the arcjet is operated in the steady mode with no voltage oscillation, and the gas flow in the arcjet thruster is axisymmetric, laminar and compressible; (ii) the velocity of each the species including electrons, follows Maxwellian distributions; (iii) the thermal nonequilibrium follows a two-temperature model that separates heavy-species temperature T_h, and the electron temperature T_e; (iv) the plasma is optically thin; (v) electron gain energy through Joule heating from the electric field and then the energy of electrons is partially transferred to heavy species through collisions.

In this study, the plasma is considered to contain electrons and heavy species of hydrogen, including molecules (H_2), atoms (H) and ions (H^+). The species productions rates, are determined as a function of T_h and T_e from the assumed finite-rate chemistry processes summarized in Table 1. The reactions chosen for this model are similar to those used in previous arcjet models[3-5]. For two-way reaction, the reverse reaction rates are extracted from the

Table 1. List of the processes considered in the model

Reaction	Rate (m^6/s or m^3/s)	Loss rate (W/m^3)
$2H+M=H_2+M$	$k_{f1}=\dfrac{1.764\times10^{-42}}{T_h}$	$L_h=\left(k_{r1}n_{H_2}-k_{f1}n_H^2\right)n_M\varepsilon_{d,H_2}$
$H^++e+M=H+M$	$k_{f2}=\dfrac{1.45\times10^{-33}}{T_h^{2.5}}$	$L_h=\left(k_{r2}n_H-k_{f2}n_{H^+}n_e\right)n_M\varepsilon_{i,H}$
$e+H_2\rightarrow 2H+e$	$k_{f3}=\langle\sigma v\rangle$	$L_e=2.34k_{f3}n_en_{H_2}\varepsilon_{d,H_2}$ $L_h=-1.34k_{f3}n_en_{H_2}\varepsilon_{d,H_2}$
$H^++e\rightarrow H+h\nu$	$k_{f4}=\dfrac{6.26\times10^{-17}}{T_h^{0.58}}$	$L_e=k_{f4}n_en_{H^+_2}\varepsilon_{i,H}$
$H^++2e=H+e$	$k_{f5}=\dfrac{1.95\times10^{-20}}{T_h^{4.5}}$	$L_e=\left(k_{r5}n_H-k_{f5}n_{H^+}n_e\right)n_e\varepsilon_{i,H}$

forward reaction and the equilibrium constants.

Fig. 1 shows the arcjet thruster used in this simulation, which has almost the same dimensions as the 1-kW-class radiation-cooled arcjet thruster designed by NASA Lewis Research Center. Due to the axisymmetry of the thruster nozzle, only the upper half is modelled in the computation. The computational domain used in the model is denoted as B-C-I-J-F-G-H-B in Fig.1, in which C-I, I-J and J-F are respectively the inner surfaces of the convergent segment, constrictor and divergent segment of the anode/nozzle.

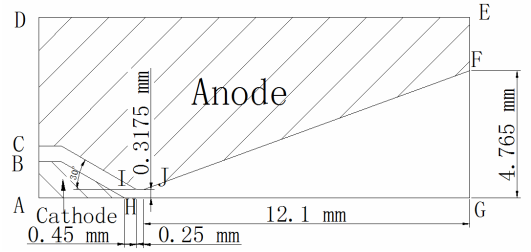

Fig. 1 Schematic diagram of the computational domain

The equations that govern the model arcjet thruster of this research are essentially a group of modified Navier-Stokes equations coupled with the Maxwell's equations. The set of governing equations in the cylindrical coordinate system can be written as follows.

$$\frac{\partial U}{\partial t}+\frac{\partial E}{\partial z}+\frac{\partial F}{\partial r}+\frac{H}{r}=\frac{\partial E_v}{\partial z}+\frac{\partial F_v}{\partial r}+\frac{H_v}{r}+S_C+S_{EM} \qquad (3)$$

Where

$$U=\begin{bmatrix}\rho\\ \rho u_z\\ \rho u_r\\ \rho e_t\\ \rho_e e_e\\ \rho f_H\\ \rho f_{H^+}\end{bmatrix};\ E=\begin{bmatrix}\rho u_z\\ \rho u_z u_z+p\\ \rho u_z u_r\\ (\rho e_t+p)u_z\\ (\rho_e e_e+p_e)u_z\\ \rho f_H u_z\\ \rho f_{H^+}u_z\end{bmatrix};\ F=\begin{bmatrix}\rho u_r\\ \rho u_z u_r\\ \rho u_r u_r+p\\ (\rho e_t+p)u_r\\ (\rho_e e_e+p_e)u_r\\ \rho f_H u_r\\ \rho f_{H^+}u_r\end{bmatrix};$$

$$H=\begin{bmatrix}\rho u_r\\ \rho u_z u_r\\ \rho u_r u_r\\ (\rho e_t+p)u_r\\ (\rho_e e_e+p_e)u_r\\ \rho f_H u_r\\ \rho f_{H^+}u_r\end{bmatrix};\ E_v=\begin{bmatrix}0\\ \tau_{zz}\\ \tau_{zr}\\ u\tau_{zz}+v\tau_{zr}-\dot q_z\\ -\dot q_{ez}\\ d_{Hz}\\ d_{H^+z}\end{bmatrix};\ F_v=\begin{bmatrix}0\\ \tau_{rz}\\ \tau_{rr}\\ u\tau_{rz}+v\tau_{rr}-\dot q_r\\ -\dot q_{er}\\ d_{Hr}\\ d_{H^+r}\end{bmatrix};$$

$$H_v=\begin{bmatrix}0\\ \tau_{rz}\\ \tau_{rr}-\tau_{\theta\theta}\\ u\tau_{rz}+v\tau_{rr}-\dot q_r\\ -\dot q_{er}\\ d_{Hr}\\ d_{H^+r}\end{bmatrix};\ S_{EM}=\begin{bmatrix}0\\ J_rB_\theta\\ -J_zB_\theta\\ J_zE_z+J_rE_r\\ J_zE_z+J_rE_r\\ 0\\ 0\end{bmatrix};$$

$$S_C=\begin{bmatrix}0\\ 0\\ 0\\ -L_e-L_h-\dot R+\frac{5}{2}\frac{k_B}{e}\left(J_x\frac{\partial T_e}{\partial z}+J_y\frac{\partial T_e}{\partial r}\right)\\ -L_e-\dot R+\frac{5}{2}\frac{k_B}{e}\left(J_x\frac{\partial T_e}{\partial z}+J_y\frac{\partial T_e}{\partial r}\right)-Q_{ech}\\ \dot n_H m_H-\dot n_{H^+}m_{H^+}\\ \dot n_{H^+}m_{H^+}\end{bmatrix};$$

and

$$\rho e_t=\frac{p}{\gamma-1}+\frac{1}{2}\rho\left(u^2+v^2\right),\ \rho_e e_e=\frac{p_e}{\gamma_e-1},\ d_{iz}=D_{a,i}\frac{\partial\rho_i}{\partial z},$$

$$d_{ir}=D_{a,i}\frac{\partial\rho_i}{\partial r},\ \dot q_z=\dot q_{ez}+\dot q_{hz},\ \dot q_r=\dot q_{er}+\dot q_{hr},$$

$$\dot q_{ez}=-D_a h_e m_e\frac{\partial n_e}{\partial z}-k_e\frac{\partial T_e}{\partial z},\ \dot q_{er}=-D_a h_e m_e\frac{\partial n_e}{\partial r}-k_e\frac{\partial T_e}{\partial r},$$

$$\dot q_{hz}=-k_h\frac{\partial T_h}{\partial z}-\sum_i D_{a,i}h_i\frac{\partial\rho_i}{\partial z},\ \dot q_{hr}=-k_h\frac{\partial T_h}{\partial r}-\sum_i D_{a,i}h_i\frac{\partial\rho_i}{\partial r},$$

$$Q_{ech}=3\rho_e\left(\frac{\nu_{eH^+}}{m_{H^+}}+\frac{\nu_{eH}}{m_H}+\delta_H\frac{\nu_{eH_2}}{m_{H_2}}\right)k_B\left(T_e-T_h\right)$$

The current distribution within an arcjet thruster is assumed to be two-dimensional, and the azimuthal current is expected to be zero. The current density is given by Ohm's law

$$\vec j=\sigma(\vec E+\vec u\times\vec B) \qquad (4)$$

Here, σ is the electric conductivity and $\vec E$ represents the electric field. Rewriting Ohm's

law by making use of Maxwell's equations for steady conditions, one obtains an equation for the magnetic induction intensity in the form[6]

$$\frac{\partial}{\partial r}\left[\frac{1}{\sigma r}\frac{\partial(rB_\theta)}{\partial r}\right]+\frac{\partial}{\partial z}\left[\frac{1}{\sigma r}\frac{\partial(rB_\theta)}{\partial z}\right]=\mu_0\left[\frac{\partial(vB_\theta)}{\partial r}+\frac{\partial(uB_\theta)}{\partial z}\right] \quad (5)$$

Here, B_θ is the azimuthal component of the magnetic induction intensity.

In this study, the Roe scheme with MUSCL limiters, a scheme for solving hyperbolic systems of conservation equations, is introduced to discretize the convection terms in equation (3), and the diffusion terms are discretized by a central differencing scheme. A forth-order Runge-Kutta scheme is chosen to march forward in time.

The Chapman-Enskog theory is used to calculate the transport properties. In the thermodynamic and chemical nonequilibrium model, the transport properties are calculated from the temperature and the composition at each position in the calculation domain for each iteration, until convergence is reached. The detailed procedure is described in reference[7].

3. RESULTS AND DISCUSSION

For the case with hydrogen as the propellant, experimental results of low power arcjet with almost the same geometrical structure, which is operated under the similar working condition with this study have been reported by Cappelli and his co-workers[8-10]. Fig. 2a and 2b compare the predicted radial distribution of the gas temperature and electron number density at the arcjet nozzle exit with corresponding experiment results for the case with hydrogen flow rates of 14.2 mg/s and arc current of 9.8 A. It is seen that the predicted results agree well with the experimental data.

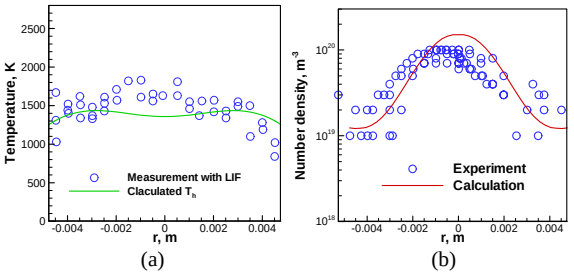

(a) (b)

Fig. 2 Comparisons of the computed results and the experimental data concerning the gas temperature (a) and number density of electron (b) profiles at the exit plane for the thruster operating at corresponding condition.

Fig. 3 compares the computed temperature of electron and heavy-species and thermal nonequilibrium parameter (T_e/T_h) along the nozzle axis within the hydrogen arcjet thruster under different working conditions. It is noted that even in the constrictor center of the nozzle, the presence of Ohmic dissipation keeps the electron temperature higher than the heavy-species temperature due to the finite collisional time scales. In the upstream of the nozzle beyond the constrictor, the flow expands and cools, but the temperature of electron decrease slower than that of heavy-species. The reason is that the electron is still heated by the arc, while the quantity of the species is not enough to support efficient coupling of energy between the electrons and heavy-species in this area. For the cases with a constant arc current, the larger mass flow rate causes the concentration of the arc core. In the smaller arc core region, the propellant is heated more rapidly, which causes the higher electron temperature and thermal nonequilibrium parameter (T_e/T_h). Fig. 3 also shows that the higher temperature can be obtained by increasing the arc current while maintain the same mass flow rate.

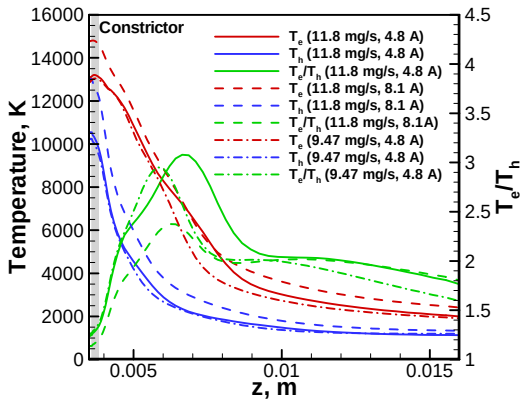

Fig. 3 Comparison of the computed temperature of electron and heavy-species and thermal nonequilibrium parameter (T_e/T_h) along the nozzle axis under three different working conditions

Fig. 4 shows the contrast of the computed mole fraction of different heavy-species along the nozzle axis under three different working conditions. It is seen that the highest degree of ionization appears in the constrictor, and the largest mole fraction of atoms is just behind the constrictor. The increase of mole fraction of atoms upstream of the divergent section is caused by the recombination of the ions due to the decrease of the temperature. Although the temperature decreases from more than 10000 K within in the constrictor to about 2000 K at the exit plane, the mole fraction of molecule and atom has not changed much. It comes to a

conclusion that degree of ionization and dissociation usually lags behind the values that would correspond to the rising or decreasing electron temperature. With a constant mass flow rate, the larger arc current could provide more power energy to increase the temperature of the plasma and the degree of ionization and dissociation. Increasing of the mass flow rate with a constant arc current could concentrate the arc core region and get the higher degree of ionization and dissociation.

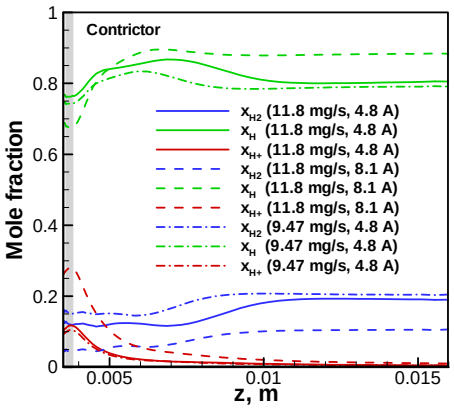

Fig. 4 Comparison of the computed mole fraction of different heavy-species along the nozzle axis under three different working conditions

4. CONCLUSION

A self-consistent nonequilibrium plasma model, comprised of 4 species and 8 reactions, has been carried out to study the effects of mass flow rate and arc current on nonequilibrium phenomenon within the arcjet with hydrogen as the propellant. Modeling results show the heavy-species temperature is about 1500 K and the electron number density is the order of 10^{19} at the exit plane, which agrees well with the experimental data. Numerical results show that considerable thermal nonequilibrium exits even in the arc core region. Increase of the mass flow rate and decrease of the arc current could cause the higher value of nonequilibrium parameter. In addition, the chemical reaction including the dissociation, ionization and recombination process, are used to take the chemical nonequilibrium effects into account, and the calculations show clearly that strong departures from dissociation and ionization equilibrium exist in the arcjet thrusters.

ACKNOWLEDGMENT

This work was supported by the National Natural Science Foundation of China. (Grant Nos. 11275021, 11072020, 50836007)

REFERENCES

[1] H. X. Wang, J. Y. Geng, X. Chen, W. X. Pan, and A. B. Murphy, "Modeling study on the flow, heat transfer and energy conversion characteristics of low-power arc-heated hydrogen/nitrogen thrusters," Plasma Chemistry and Plasma Processing, **30**, 707, 2010.

[2] H. X. Wang, F. Z. Wei, A. B. Murphy, and Y. Liu, "Numerical Investigation of the Plasma Flow Through the Constrictor of Arc-Heated Thrusters," Journal of Physics D: Applied Physics, **45**, 235202, 2012.

[3] T. W. Megli, "A nonequilibrium plasma-dynamics model for nitrogen/hydrogen arcjets," Ph.D. Dissertation, Mechanical Engineering Dept., University of Illinois at Urbana-Champaign, Urbana, Illinois, 1995.

[4] S. A. Miller, "Multifluid nonequilibrium simulation of arcjet thrusters," Ph.D. Dissertation, Aeronautics and Astronautics Dept., Massachusetts Institute of Technology, Cambridge, MA, 1994.

[5] D. Keefer, D. Burtner, T. Moeller, and R. Rhodes, "Multiplexed Laser Induced Fluorescence and Non-Equilibrium Processes in Arcjets," 25th AIAA Plasmadynamics and Lasers Conference, Colorado Springs, CO, 1994-AIAA-94-2656.

[6] P. C. Sleziona, M. Auweter-Kurtz, and H. O. Schrade, "Numerical calculation of nozzle type and cylindrical MPD thrusters," 28th AIAA/ASME/SAE/ASEE Joint Propulsion Conference and Exhibit, Nashville, TN, 1992 - AIAA-92-3296.

[7] A. B. Murphy, "Transport Coefficients of Hydrogen and Argon-Hydrogen Plasma," Plasma Chemistry and Plasma Processing, **20**, 279, 2000.

[8] P. V. Storm, and M. A. Cappelli, "LIF Characterization of Arcjet Nozzle Flow," 32nd AIAA/ASME/SAE/ASEE Joint Propulsion Conference and Exhibit, Lake Buena Vista, FL, 1996-AIAA-96-2987.

[9] J. G. Liebeskind, R. K. Hanson, and M. A. Cappelli, "Laser-Induced Fluorescence Diagnostic for Temperature and Velocity Measurements in a Hydrogen Arcjet Plume," Applied optics, **32**, 6117, 1993.

[10] P. V. Storm, and M. A. Cappelli, "Stark Broadening Corrections to Laser-Induced Fluorescence Temperature Measurements in a Hydrogen Arcjet Plume," Applied optics, **35**, 4913, 1996.